Optical Measurement of Presynaptic Calcium Currents

Bernardo L. Sabatini and Wade G. Regehr
Department of Neurobiology, Harvard Medical School, Boston, Massachusetts 02115 USA

ABSTRACT Measurements of presynaptic calcium currents are vital to understanding the control of transmitter release. However, most presynaptic boutons in the vertebrate central nervous system are too small to allow electrical recordings of presynaptic calcium currents (I_{Ca}^{pre}). We therefore tested the possibility of measuring I_{Ca}^{pre} optically in boutons loaded with calcium-sensitive fluorophores. From a theoretical treatment of a system containing an endogenous buffer and an indicator, we determined the conditions necessary for the derivative of the stimulus-evoked change in indicator fluorescence to report I_{Ca}^{pre} accurately. Matching the calcium dissociation rates of the endogenous buffer and indicator allows the most precise optical measurements of I_{Ca}^{pre}. We tested our ability to measure I_{Ca}^{pre} in granule cells in rat cerebellar slices. The derivatives of stimulus-evoked fluorescence transients from slices loaded with the low-affinity calcium indicators magnesium green and mag-fura-5 had the same time courses and were unaffected by changes in calcium influx or indicator concentration. Thus both of these indicators were well suited to measuring I_{Ca}^{pre}. In contrast, the high-affinity indicator fura-2 distorted I_{Ca}^{pre}. The optically determined I_{Ca}^{pre} was well approximated by a Gaussian with a half-width of 650 μs at 24°C and 340 μs at 34°C.

INTRODUCTION

Classic studies at the squid giant synapse and the frog neuromuscular junction established that calcium plays a central role in triggering neurotransmitter release (Dodge and Rahamimoff, 1967; Jenkinson, 1957; Katz and Miledi, 1967). Action potential invasion of presynaptic terminals provides the depolarization to open voltage-gated calcium channels through which calcium enters the cell and triggers vesicle fusion (see Schweizer et al., 1995, for a review). In trying to understand how the presynaptic waveform determines the time course and magnitude of calcium entry, and how calcium channels are coupled to the release apparatus, it is necessary to have a measure of the presynaptic calcium current. Initially this was possible only at a few synapses, such as the squid giant synapse, whose immense size made it suited to electrophysiological techniques (Augustine and Eckert, 1984; Llinas et al., 1981). More recently, presynaptic calcium currents have also been recorded in some particularly large boutons in the vertebrate central nervous system with whole-cell voltage clamp (Borst and Sakmann, 1996; Martin et al., 1989; Sivaramakrishnan and Laurent, 1995; Stanley, 1989; Yawo, 1990).

However, most presynaptic boutons in the vertebrate central nervous system are too small to allow direct recording of calcium currents with an electrode, and other approaches must be used. One possibility is to use optical methods. In several slice preparations it is possible to load the presynaptic boutons of an axonal projection with fluorescent calcium indicators (Regehr and Atluri, 1995; Regehr and Tank, 1991; Wu and Saggau, 1994). This suggests an approach to measuring presynaptic calcium currents that is summarized in Fig. 1 (Kao and Tsien, 1988; Neher, 1995; Sabatini and Regehr, 1996, 1997; Sinha et al., 1997). Stimulation of the axon generates an action potential that invades a presynaptic bouton and evokes a calcium current. Entering calcium rapidly equilibrates with calcium-binding proteins within the presynaptic bouton and is then extruded from the terminal on a slower time scale. In presynaptic boutons in which a calcium-sensitive fluorophore has been introduced, calcium will also bind to the fluorophore and alter its fluorescence properties. If conditions can be found in which the rate of calcium binding by the indicator is proportional to the calcium current, then the rate of change of fluorescence will provide an accurate measure of the time course of the calcium current. However, many factors can prevent the accurate detection of presynaptic calcium currents with this approach and, as in Fig. 1, the time course of the rate of fluorescence change of a calcium indicator might not perfectly track the presynaptic calcium current.

Here we use a combination of experimental and theoretical approaches to assess the feasibility of optically measuring calcium currents. A computer model of calcium buffering and diffusion in the presynaptic terminal was used to predict the kinetics of calcium binding to an indicator in response to action potential-triggered calcium influx. We examined the effects of a number of factors on our ability to measure calcium currents, including the properties of the calcium indicator and the endogenous calcium buffer; interactions between the indicator and the endogenous buffer; and diffusion of calcium and the buffers within the bouton. We used the model to develop assays of the accuracy of optically measured calcium currents and examined our ability to measure presynaptic calcium currents from granule cell parallel fibers in slices from rat cerebellum. We found that, for cerebellar granule cell presynaptic boutons, low-affinity calcium indicators accurately report the time course

Received for publication 18 September 1997 and in final form 1 December 1997.

Address reprint requests to Dr. Wade Regehr, Department of Neurobiology, Harvard Medical School, 220 Longwood Ave., Boston, MA 02115. Tel.: 617-432-0435; Fax: 617-734-7557; wregehr@warren.med.harvard.edu.

0006-3495/98/03/1549/15 $2.00

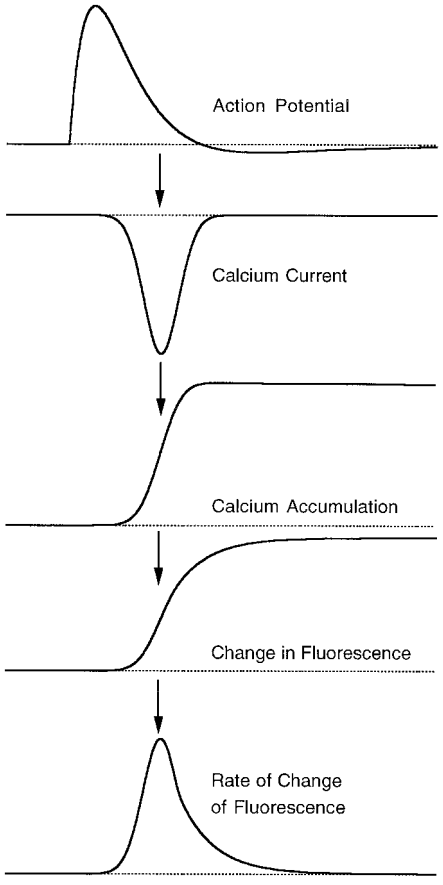

FIGURE 1 Schematic showing the basis for optical measurement of presynaptic calcium currents. Depolarization of the presynaptic bouton opens voltage-gated calcium channels, resulting in a calcium current and the accumulation of calcium. If the bouton contains a calcium-sensitive indicator, this will in turn produce a change in fluorescence. Here we determine the conditions for which the time course of the rate of change of fluorescence provides a good estimate of the time course of the presynaptic calcium current.

of presynaptic calcium currents as well as the timing of calcium entry.

METHODS

Transverse slices (300 μm thick) were cut from the cerebellar vermis of 14–20-day-old Sprague-Dawley rats. The slices were allowed to recover at 30°C for 1 h before use. The external solution consisted of (in mM) 125 NaCl, 2.5 KCl, 2 $CaCl_2$, 1 $MgCl_2$, 26 $NaHCO_3$, 1.25 NaH_2PO_4, 25 glucose, and 0.02 bicuculline, bubbled with 95% O_2 and 5% CO_2.

Detection of presynaptic calcium transients

Parallel fibers were labeled with a high-pressure stream of mag-fura-5 (Delbono and Stefani, 1993; Zhao et al., 1996), magnesium green (Atluri and Regehr, 1996; Zhao et al., 1996), or fura-2 (Grynkiewicz et al., 1985), using techniques developed previously (Regehr and Atluri, 1995; Regehr and Tank, 1991). All indicators were obtained from Molecular Probes (Eugene, OR). Epifluorescence was measured with a photodiode from a spot several hundred microns from the loading site, where most of the fluorescence signal arises from parallel fiber presynaptic boutons that synapse onto Purkinje cells (Regehr and Atluri, 1995). For fura-2 and mag-fura-5 experiments, illumination from a 150-W xenon bulb was passed through a 395/35 nm (Chroma, Brattleboro, VT) excitation filter, a 420 DCLP dichroic (Chroma), and, on the emission side, a 455 LP filter and BG22 broad-band filter (Chroma) was used. For magnesium green experiments, illumination from a 100-W tungsten bulb powered by a low-noise DC power supply (no. 6542A; Hewlett Packard, Palo Alto, CA) was passed through a 450–490-nm (Zeiss, Germany) excitation filter (515 DRLP dichroic) and a 530 LP filter. In experiments in which magnesium green and mag-fura-5 were coloaded, a 380 DF15 excitation filter was used for mag-fura-5 to minimize excitation of magnesium green when mag-fura-5 fluorescence was recorded. Illumination was gated by a TTL pulse controlling an electromechanical shutter (Vincent Associates, Rochester, NY), and the area of illumination was restricted by an iris diaphragm. Unless otherwise indicated, all filters and dichroics were purchased from Omega Optical (Brattleboro, VT). At these excitation wavelengths, increases in calcium binding correspond to decreases in fluorescence for mag-fura-5 and fura-2, and to increases in fluorescence for magnesium green. Fura-2 and mag-fura-5 fluorescence transients have been inverted for clarity.

Simultaneous recordings of presynaptic waveform and calcium currents

Slices were focally loaded with magnesium green, followed by bath loading with the voltage-sensitive dye RH482 (50–100 μg/ml for 0.5–1 h). RH482 has been used previously to record parallel fiber action potential waveforms in cerebellar slices (Konnerth et al., 1987; Sabatini and Regehr, 1996, 1997). Illumination from two tungsten bulbs was combined by using a 710 DF20 filter, a 450–490-nm filter (Zeiss), and a 515 DRLP dichroic, and passed through a custom 490/700 DBDR dichroic. Transmitted light was filtered through a second 710 DF20 and monitored with a photodiode placed below the condenser while epifluorescence was collected (10SWF-650, Newport, Irvine, CA, and LP530 filters) and focused onto a second photodiode. Stimulus-evoked RH482 transmittance transients show a sustained component that may represent depolarization of both stimulated and unstimulated parallel fibers caused by accumulation of extracellular potassium (Kocsis et al., 1983; Sabatini and Regehr, 1997).

Electrophysiology

Whole-cell recordings of stellate cells were obtained by using 2.0–2.6-MΩ glass pipettes containing an internal solution of (in mM) 35 CsF, 100 CsCl, 10 EGTA, 10 HEPES, 0.1 D600 (pH 7.3) with CsOH (Regehr and Mintz, 1994; Sabatini and Regehr, 1996). Parallel fibers were stimulated with 0.1-ms current pulses delivered to the molecular layer via a glass electrode. EPSCs were recorded with an Axopatch 200A (Axon Instruments, Foster City, CA) in voltage clamp mode. Series resistance was not compensated.

Data collection and digital processing

Data were recorded with an A/D converter (Instrutech, Great Neck, NY) and a Macintosh computer running Igor Pro (Wavemetrics, Lake Oswego, OR) and PULSE CONTROL software (Herrington and Bookman, 1995). Derivatives were calculated digitally, using a difference approximation that introduced no time delays. Digital filtering was accomplished by multiplying, in Fourier space, the fluorescence transient with a low-pass Bessel filter, $H(\omega) = 1/(1 + (\omega/\omega_c)^{2n})$, where ω_c is the corner frequency of the filter and n is the number of poles. Typically an 8-pole filter was used, and this procedure did not introduce time delays.

Simulations of calcium transients

Simulations of calcium diffusion and buffering in the presynaptic terminal were performed using Igor Pro. The differential equations describing

calcium buffering and diffusion are

$$\frac{\partial[\mathrm{BCa}]}{\partial t} = k_+^{\mathrm{B}}[\mathrm{Ca}][\mathrm{B}] - k_-^{\mathrm{B}}[\mathrm{BCa}] \quad (1)$$

$$\frac{\partial[\mathrm{FCa}]}{\partial t} = k_+^{\mathrm{F}}[\mathrm{Ca}][\mathrm{F}] - k_-^{\mathrm{F}}[\mathrm{FCa}] \quad (2)$$

$$\frac{\partial[\mathrm{Ca}]}{\partial t} = -\frac{\partial[\mathrm{BCa}]}{\partial t} - \frac{\partial[\mathrm{FCa}]}{\partial t} + \frac{i_{\mathrm{Ca}}(t)}{2FV} \quad (3)$$

$$J_{\mathrm{X}} = -D_{\mathrm{X}}\frac{\partial[\mathrm{X}]}{\partial x} \quad (4)$$

where $i_{\mathrm{Ca}}(t)$ is the calcium current as a function of time, F is Faraday's constant, V is the volume of the compartment receiving the calcium influx, J_{X} is the flux of species X per unit area per unit time, and D_{X} is the diffusion coefficient of species X (Crank, 1975). See Table 1 for the definition of the remainder of the terms. Using the relationships

$$[\mathrm{Ca}]_{\mathrm{tot}} = [\mathrm{Ca}] + [\mathrm{BCa}] + [\mathrm{FCa}] \quad (5)$$

$$[\mathrm{B}]_{\mathrm{tot}} = [\mathrm{B}] + [\mathrm{BCa}] \quad (6)$$

$$[\mathrm{F}]_{\mathrm{tot}} = [\mathrm{F}] + [\mathrm{FCa}] \quad (7)$$

the system of differential equations was solved numerically, using fifth-order Runge-Kutta-Fehlberg numerical integration with an embedded adaptive time step (Press et al., 1992).

The presynaptic terminal was represented as a 1-μm-diameter sphere that was modeled either as a single compartment or, when the effects of diffusion were considered, as 10 concentric shells of 50 nm thickness. The calcium current was chosen to be a Gaussian with a standard deviation of 0.4 ms at 24°C or 0.2 ms at 34°C, corresponding to a width at half-maximum of 670 μs and 335 μs, respectively. Kinetic parameters for the calcium indicators are listed in Table 1. Although we cannot measure the affinity of the indicators in granule cell presynaptic terminals, the relative affinities were monitored by the saturation of the $\Delta F/F$ response during a train of stimuli (Regehr and Atluri, 1995; Sabatini and Regehr, 1995). Fura-2 showed significant saturation by the second stimulus, saturation of magnesium green was clear after three or four stimuli, whereas mag-fura-5 showed little saturation over a train of 10 stimuli.

Parameters in the model

Studies of calcium buffering in various cell types have pointed to the importance of endogenous calcium buffers in determining the time course and spatial localization of intracellular calcium signaling (Fogelson and Zucker, 1985; Neher and Augustine, 1992; Roberts, 1993, 1994; Simon and Llinas, 1985; Zhou and Neher, 1993). Because the concentration and kinetic parameters of the calcium buffers present in the presynaptic terminals of granule cells are not known, we tested many different parameter combinations for their ability to reproduce, in the numerical model, our experimental data.

In the differential equations that govern the calcium buffering dynamics (Eqs. 1–3), the calcium association rates of the buffers always appear as products with a concentration, and, therefore, an infinite number of parameter combinations result in the same time course of calcium buffering. To remove this indeterminacy, we used reported values for the calcium association rates of fura-2 and the endogenous buffer (see Table 1).

The calcium affinity of the endogenous buffer was allowed to vary from 1 to 150 μM and its concentration from 1 to 1000 times its K_{d}. The calcium current amplitude and the fura-2 concentration were calculated for each combination of the above parameters for the model to accurately reproduce two features of the experimental data: 1) two stimuli delivered in rapid succession to parallel fibers loaded with fura-2 results in a $\Delta F/F$ signal that is 40% larger than that produced by a single stimulus; and 2) the 50–100% rising phase of the fura-2 fluorescence transient can be approximated by an

TABLE 1 Definitions and values of parameters used in the numerical model

Symbol	Definition	Value	
		24°C	34°C
[Ca]	Concentration of free calcium	50 nM at rest	50 nM at rest
$[\mathrm{B}]_{\mathrm{tot}}$	Total concentration of endogenous buffer	2 mM	2 mM
[B]	Concentration of unbound endogenous buffer		
k_+^{B}	Calcium association rate of endogenous buffer	1×10^8 $\mathrm{M}^{-1}\mathrm{s}^{-1}$*	2×10^8 $\mathrm{M}^{-1}\mathrm{s}^{-1}$#
$K_{\mathrm{d}}^{\mathrm{B}}$	Calcium affinity of endogenous buffer	50 μM	50 μM
$[\mathrm{F}]_{\mathrm{tot}}$	Concentration of calcium indicator	30 μM	30 μM
[F]	Concentration of unbound indicator		
k_+^{F}	Calcium association rate of indicator	5×10^8 $\mathrm{M}^{-1}\mathrm{s}^{-1}$*§	1.4×10^9 $\mathrm{M}^{-1}\mathrm{s}^{-1}$¶
$K_{\mathrm{d}}^{\mathrm{F}}$	Calcium affinity of the calcium indicator		
	Fura-2	200 nM*§	107 nM¶
	Magnesium green	7 μM‖**	3.8 μM¶
	Mag-fura-5	20 μM	10.7 μM¶
k_-^{X}	Calcium dissociation rate of buffer X	$K_{\mathrm{d}}^{\mathrm{X}}k_+^{\mathrm{X}}$	
[CaX]	Concentration of calcium bound form of X		
ν_{X}	Equilibration rate of buffer X after a step increase in calcium when no other buffers are present	$k_-^{\mathrm{X}} + k_-^{\mathrm{X}}([\mathrm{Ca}]_\infty + [\mathrm{X}]_\infty)$§	
ν_{slow}, ν_{fast}	Slow and fast equilibration rate governing dynamics of a two-buffer system following a step increase in calcium	See Appendix	
$[\mathrm{X}]_{\mathrm{o}}$, $[\mathrm{X}]_\infty$	Concentration of X at rest or at steady state		

*Xu et al. (1997).
#Derived from value at 24°C by requiring our model to reproduce 34°C fura-2 fluorescence transients.
§Kao and Tsien (1988).
¶Calculated from corresponding value at 24°C using the Q_{10}'s in Kao and Tsien (1988).
‖Zhao et al. (1996).
**Haugland (1996).

exponential with a time constant of 2.9 ms. To match these features, the amplitude of the calcium current was set such that doubling the amount of calcium entering the terminal increased Δ[CaFura] by 40%, and the concentration of fura-2 was chosen such that $\nu_{slow} = (2.9\ ms)^{-1}$ (see Appendix). Each parameter set for which these calculations gave physically meaningful results (i.e., $i_{Ca} > 0$ and $[F]_{tot} > 0$) was tested in the numerical simulation. The amplitude of the calcium current ranged from 1 to 100 pA, and the concentration of fura-2 from 2 to 1500 μM.

Fig. 2 shows the outcome of such a parameter search. With the parameters listed in Table 1, the numerical model results in a very close match to the fura-2 fluorescence transient measured at 24°C and its derivative. In addition, with these parameters the model accurately reproduces the effect of lowering extracellular calcium on the fura-2 fluorescence transient (see Fig. 6). Under these conditions, the derivatives of the magnesium green or mag-fura-5 fluorescence transients provide accurate measures of the time course of the calcium current.

We can graphically depict the dependence of these fits on the model parameters by plotting the RMS difference between the output of the numerical model and the recorded fura-2 transients as a function of the calcium affinity of the endogenous buffer and the endogenous buffer capacity (defined as $[B]_{tot}/K_d$) (Fig. 2). A large number of parameter combinations result in good fits to the shape of the fura-2 transient and its derivative. For endogenous buffer affinities of 20–70 μM, the output of the numerical simulation matches both the fura-2 transient and its derivative with an average RMS error of less than 1%. In the region defined by buffer capacities greater than 10 and endogenous buffer affinities of 30–70 μM, the model also predicts that the time courses of magnesium green and mag-fura-5 fluorescence transients will be similar and accurately report the time course of the calcium current. The relatively low buffer capacity is similar to that reported previously for chromaffin cells and calyceal synapses (Helmchen et al., 1997; Zhou and Neher, 1993) and less than that reported for hair cells, crayfish nerve terminals, and rod outer segments (Lagnado et al., 1992; Roberts et al., 1990; Tank et al., 1995). The calcium affinity of the endogenous buffer is similar to that reported for chromaffin cells (Xu et al., 1997).

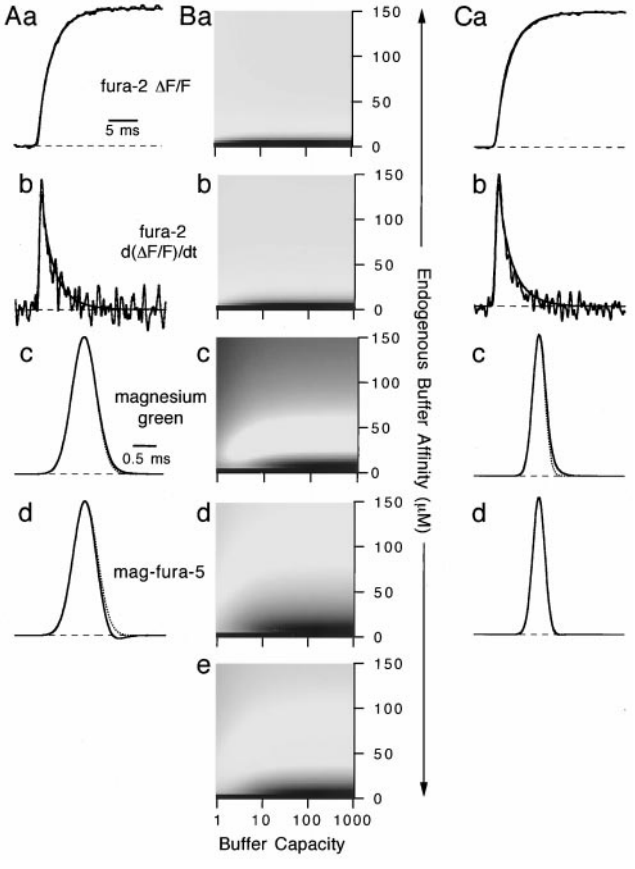

FIGURE 2 Estimation of parameters used in simulations. (*a*) Stimulus-evoked fura-2 fluorescence transient (*noisy trace*) and [CaF] predicted by the numerical model (*solid line*). (*b*) Derivatives of the traces shown in *a*. (*c* and *d*) d[CaF]/d*t* (*solid line*) predicted by the model for magnesium green (*c*) and for mag-fura-5 (*d*) compared to the calcium current (*dotted line*). Experiments were performed at 24°C (*A*) or 34°C (*C*), and the default model parameters appropriate for each temperature were used. (*B*) (*a–d*) Average percentage RMS difference between the two traces shown in the corresponding panel of *A*, as generated by the simulation for a range of calcium affinities and capacities of the endogenous buffer. (*e*) Average of the percentage RMS differences shown in *a–d*. White represents an average difference of 1%, 1%, 3%, 2%, and 2%, and black a difference of 4%, 6%, 9%, 20%, and 14% in *a–e*, respectively.

High temperature parameters

Parameters for the model at 34°C were determined by again constraining the model to match our experimental data. The endogenous buffer and the calcium indicator concentrations were maintained at the values determined by our parameter search for the 24°C model. To adjust for the higher temperature, the association and dissociation rates of fura-2 were accelerated using the published values for the Q_{10} of similar indicators (Kao and Tsien, 1988). We varied the Q_{10} of the association and dissociation rates of the endogenous buffer separately until a good fit was obtained to the fura-2 fluorescence transients measured at 34°C (Fig. 2 *C*). With these parameters, magnesium green and mag-fura-5 fluorescence transients had the same time course, and their derivatives accurately reported the time course of the presynaptic calcium current.

RESULTS

Dependence of fluorescence transients on indicator properties

The first step in this study was to measure the response of calcium-sensitive indicators in granule cell parallel fibers to single stimuli delivered to the molecular layer. These fibers consist of a series of presynaptic boutons joined by thin axons, and an estimated 80% of the volume of these structures is due to presynaptic boutons (Palay and Chan-Palay, 1974). We have previously shown that stimulus-evoked fluorescence changes from parallel fibers loaded with calcium-sensitive fluorophores are triggered by calcium entering the presynaptic terminal through voltage-gated calcium channels opened by a propagating action potential (Mintz et al., 1995; Regehr and Atluri, 1995). We found that the time course of the fluorescence transient depended on the properties of the indicator used (see Table 1). The rate of rise of the $\Delta F/F$ is slowest for fura-2 and faster for the lower affinity indicators, magnesium green and mag-fura-5 (Fig. 3). The average half-widths of the derivatives of the fluorescence transients were 1450 ± 125, 640 ± 30, and 620 ± 35 μs (average ± SEM, $n = 5$), respectively, for fura-2, magnesium green, and mag-fura-5-labeled slices at 24°C. Fig. 3 *A* also shows an experiment in which mag-fura-5 and magnesium green were loaded together into the parallel fibers and the response of each dye was measured sequentially. The fluorescence transients produced by these two dyes have indistinguishable time courses.

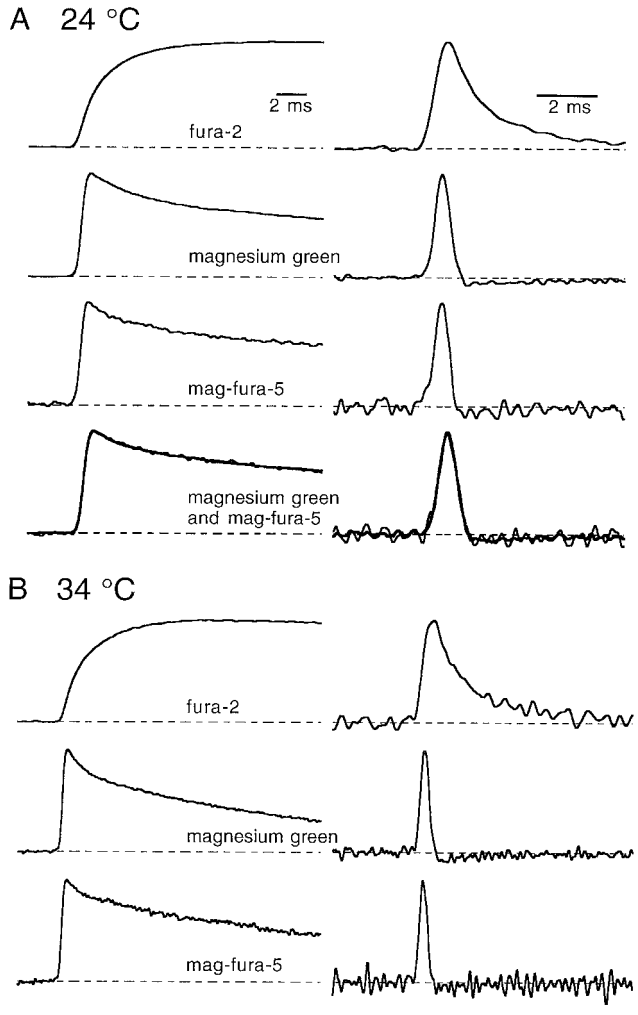

FIGURE 3 Comparison of stimulus-evoked fluorescence transients recorded from parallel fibers loaded with different calcium indicators. (*A*) The fluorescence transients (*left*) and their derivatives (*right*), recorded after stimulation of parallel fibers labeled with the indicated calcium dyes at 24°C (*A*) and 34°C (*B*). In *A*, the bottom panel shows an experiment in which mag-fura-5 (*thin trace*) and magnesium green (*thick trace*) fluorescence transients were recorded sequentially from parallel fibers loaded with both dyes.

At 34°C the time courses of the fluorescence changes were accelerated (Fig. 3 *B*). The half-widths of the derivatives of the fluorescence transients were 1050 ± 100, 340 ± 20, and 330 ± 30 μs (average ± SEM, $n = 5$), respectively, for fura-2, magnesium green, and mag-fura-5-labeled slices. Thus, as was also the case at lower temperatures, the time courses of magnesium green and mag-fura-5 fluorescence transients were indistinguishable, but were faster than that of fura-2.

Simulations examining the effects of diffusion

We performed a series of simulations to evaluate the fidelity with which the derivatives of the fluorescence changes track the presynaptic calcium current. We began by analyzing the effects of diffusion on the kinetics of calcium binding to the indicator by performing simulations with the presynaptic bouton subdivided into 10 concentric shells, each 50 nm thick. Calcium influx and extrusion were assumed to occur uniformly throughout the surface of the outermost shell. Models of this sort have been widely used to simulate calcium transients in neurons (Blumenfeld et al., 1992; Connor and Nikolakopoulou, 1982; Grisell and Andresen, 1979; Nowycky and Pinter, 1993; Sala and Hernandez-Cruz, 1990; Smith and Zucker, 1980). As seen in Fig. 4 *A*, this model predicts that large calcium gradients exist within the bouton that outlast the calcium current by several milliseconds. However, the time courses of the volume average of the calcium bound form of fura-2, [CaFura], and its derivative, d[CaFura]/d*t*, are not substantially different from those predicted by the one-compartment model (Fig. 4 *B*). Similar results were found for magnesium green and mag-fura-5 (Fig. 4, *C* and *D*), indicating that the presence of concentration gradients within the presynaptic terminal does

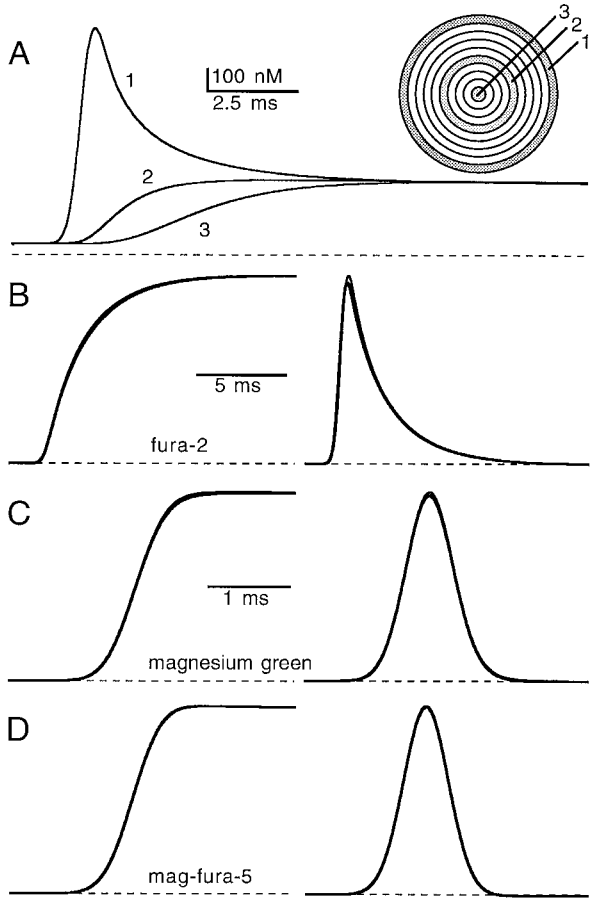

FIGURE 4 Simulations of the effects of diffusion and spatial gradients on $\Delta F/F$ signals. (*A*) Calcium concentrations in the outer, middle, and inner shells of a 10-shell model of the presynaptic terminal. (*Inset*) Schematic of the model and position of the three shells. Volume-averaged [CaF] (*left*) and d[CaF]/dt (*right*) from a 10-shell model (*thin trace*) and from a one-compartment model (*thick trace*) for indicators with properties corresponding to fura-2 (*B*), magnesium green (*C*), or mag-fura-5 (*D*). Default parameters for 24°C were used. The diffusion coefficients used were 6×10^{-6}, 1×10^{-6}, and 0 $cm^2\ s^{-1}$ for free calcium, the indicator, and the endogenous buffer, respectively.

not significantly affect the kinetics of calcium binding to calcium indicators. It follows that the effects of diffusion could be disregarded for the range of parameters used in this study. This is an important conceptual simplification when trying to understand the properties of calcium-indicator binding. For the remainder of the paper, a simplified model is used in which the presynaptic terminal is represented by a single compartment.

Simulations of calcium binding to one buffer

We next examined the properties of calcium transients when only a single calcium indicator and no endogenous buffers were present in the terminal. Simulations were performed for several indicators with properties corresponding to those of fura-2, magnesium green, and mag-fura-5 (Fig. 5 *A*). These simulations show that the time course of [CaFura] depends on the amount of fura-2 present. For the lowest concentrations of fura-2, there is a delay between calcium influx and the rise in [CaFura], but as the fura-2 concentration is increased, [CaFura] rises more quickly and has a time course closer to the integral of the calcium current. A comparison of the calcium current to the derivative of [CaFura] shows that ~100 μM fura-2 is needed before the two have similar time courses. On the other hand, for the lower affinity indicators, magnesium green and mag-fura-5 (Fig. 5 *Ac*), 1 μM of the indicator follows calcium influx with a lag of just 50 μs, and further increasing their concentrations only slightly accelerates the kinetics of calcium binding.

These results are easily explained by considering the analytical solution to the rate of accumulation of the calcium-bound form of the fluorophore, [CaF], after a small step increase in total calcium. [CaF] will increase to its equilibrium value with an exponential time course with a rate given by (Kao and Tsien, 1988)

$$v_F = k_- + k_+([F]_\infty + [Ca]_\infty) \quad (8)$$

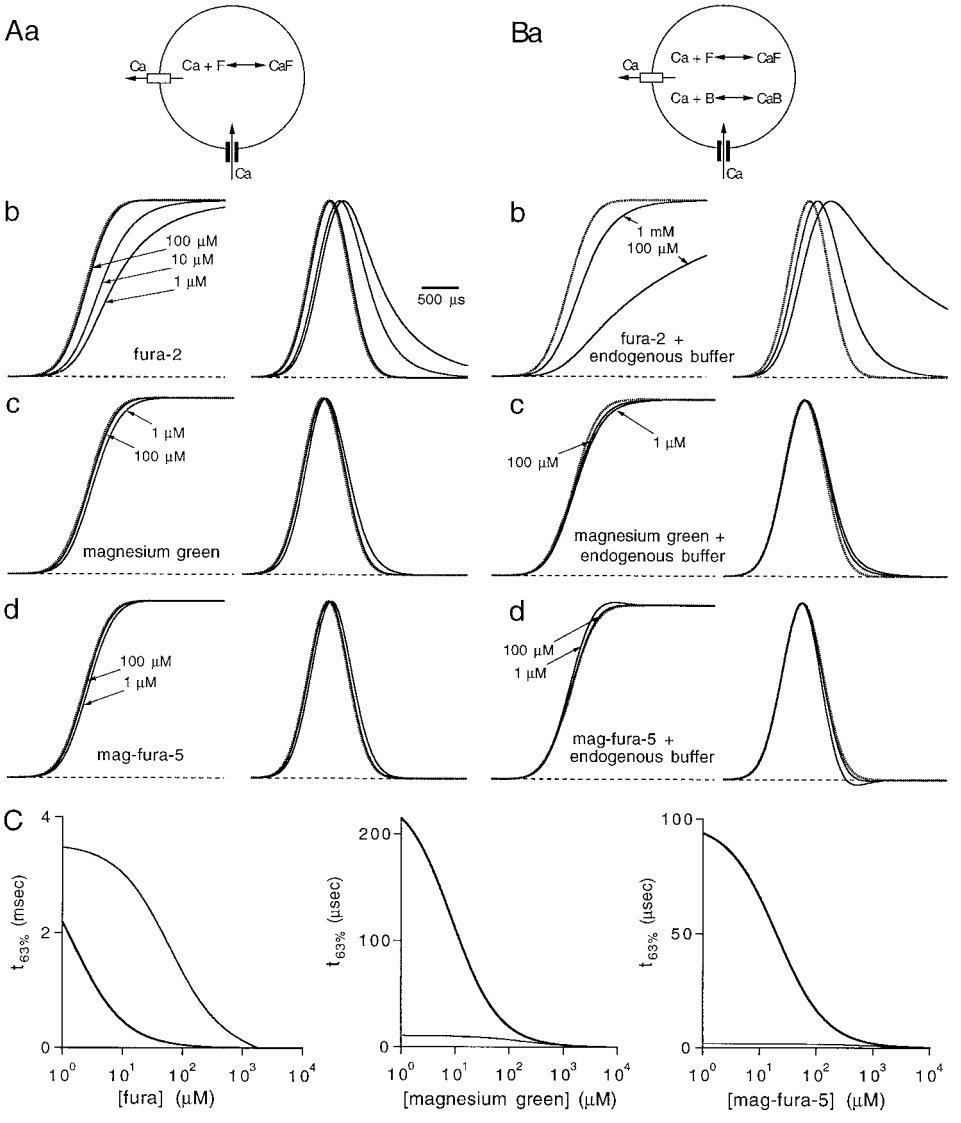

FIGURE 5 The dependence of the kinetics of calcium binding to an indicator on the concentrations of the endogenous buffer and the indicator. Simulations of calcium interacting with an indicator in a one-compartment model in which the presynaptic terminal contained the fluorophore alone (*A*) or both the fluorophore and an endogenous calcium buffer (*B*). Calcium indicators with the properties of fura-2 (*a*), magnesium green (*b*), or mag-fura-5 (*c*) were used in the simulations. The left panel shows the indicator-calcium binding (*solid lines*) and the integral of the calcium current (*dotted trace*). Each trace is labeled with the concentration of indicator used in the simulation. On the right are shown the normalized derivatives of the traces on the left (*solid lines*) and the true calcium current (*dotted trace*). (*C*) Sixty-three percent rise time of [CaF] for fura-2, magnesium green, or mag-fura-5 alone (*thick line*) or in the presence of an endogenous buffer (*thin line*). Default parameters for 24°C were used.

With vanishingly low concentrations of unbound indicator and free calcium, the equilibration rate is k_-, and equilibrium is reached more rapidly as the indicator concentration is increased. For this reason, lower affinity indicators, which have higher off rates, respond rapidly, even when present at low concentrations, whereas fura-2, which has a slow off rate, needs to be present at high concentrations to equilibrate quickly with calcium (Fig. 5 *C*).

Simulations of calcium binding to two buffers

The addition of a second calcium buffer complicates the kinetics of the indicator-calcium interaction (Fig. 5 *B*; see Table 1 for parameters). The response of fura-2 is dramatically slowed by including the endogenous calcium buffer in the model, such that even 1 mM fura-2 cannot accurately follow the time course of calcium influx. In contrast, magnesium green and mag-fura respond more rapidly in the presence of the endogenous buffer, such that just 1 μM of these indicators responds almost instantly to changes in calcium concentration. For both indicators, d[CaF]/d*t* provides a good approximation of the time course of the calcium current, although there is a slight overshoot on the decay phase of the derivative for low concentrations of mag-fura-5. The effects of endogenous buffers on the response time of the various indicators are summarized in Fig. 5 *C*. These simulations suggest that the presence of an endogenous buffer can reduce the response time of low-affinity indicators, thereby aiding in the detection of presynaptic calcium currents. However, the same endogenous buffer hinders the detection of calcium currents with fura-2. The complexities of the interactions of calcium with the endogenous buffer and the calcium indicator are explored in the Appendix and summarized in the Discussion.

The dependence of d($\Delta F/F$)/d*t* on calcium and indicator concentrations

A test of the contribution of indicator kinetics to the time course of the fluorescence signal was made by examining the effects of changing calcium influx or indicator concentration on the rate of rise of the fluorescence signals. Equation A1 predicts that if the time course of the fluorescence signal is limited by the kinetics of the calcium binding reaction of the indicator, then manipulating the intracellular free calcium or indicator concentration will alter the shape of the fluorescence signal. When $[Ca]_\infty$ is greater than or comparable to $[F]_\infty$, d($\Delta F/F$)/d*t* will be affected by changes in calcium influx. Conversely, when $[F]_\infty$ is greater than or comparable to $[Ca]_\infty$, d($\Delta F/F$)/d*t* will be affected by changes in indicator concentration. Whenever the rate of rise of the fluorescence signal is limited by calcium binding kinetics, it will be affected by at least one of these manipulations.

Under normal conditions the concentration of unbound indicator will be much greater than that of the free calcium, and therefore reducing the calcium influx will have only small effects on the time course of the fluorescence transient. At 24°C, reducing the calcium influx by lowering external calcium (Mintz et al., 1995) slightly slowed the time course of fura-2 fluorescence transients, but had no effect on the time course of magnesium green fluorescence transients (Fig. 6 *A*). At 34°C, this manipulation did not alter the time course of the fluorescence transient of either of these indicators (Fig. 6 *B*). It appears that at 34°C the calcium influx is greatly reduced and plays a smaller role in determining the fura-2 calcium binding kinetics.

Changing indicator concentration is a more sensitive test of the contribution of indicator kinetics to the time course of the fluorescence signal. We therefore compared the shape of fluorescence transients from experiments in which we loaded dye for only 5 min to the shape of fluorescence transients from experiments in which we loaded for more than 30 min. Fiber tracts labeled for longer were much brighter, and showed slower rates of fluorescence decay (on a time scale of hundreds of milliseconds), consistent with higher indicator concentrations. As shown in Fig. 7, at 24°C the rate of rise of the fluorescence signal is affected by the degree of loading for fura-2, but not for magnesium green or mag-fura-5. At 34°C the time course was affected by the

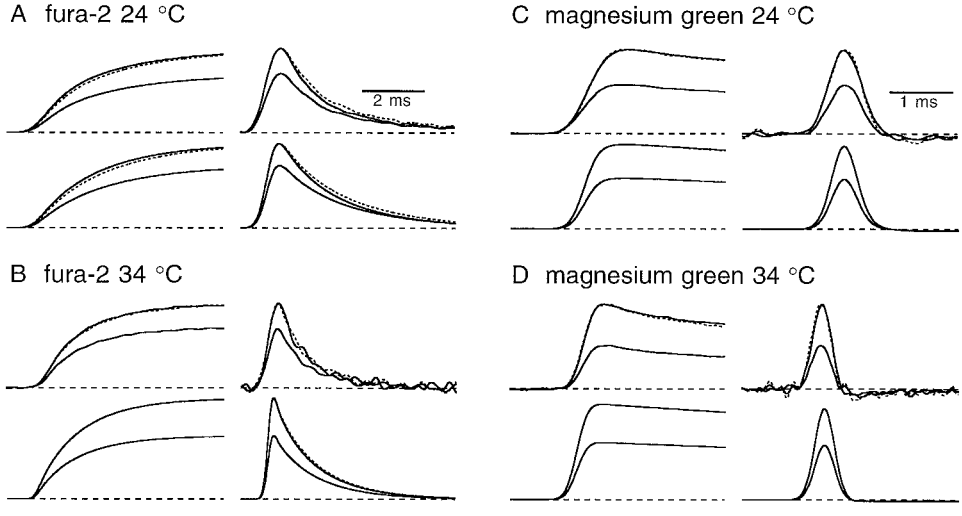

FIGURE 6 Effects of decreasing calcium influx on the kinetics of calcium binding to the indicator. Fluorescence transients (*top left panels*) and corresponding simulations (*bottom left panels*) in 2 mM and 1 mM external calcium for fura-2 (*A*, *B*) and magnesium green (*C*, *D*) at 24°C (*A*, *C*) and 34°C (*B*, *D*). The right panels show the derivatives of the traces on the left, and in all panels, the dotted trace is the trace in 1 mM Ca_e normalized to the amplitude of the 2 mM Ca_e trace.

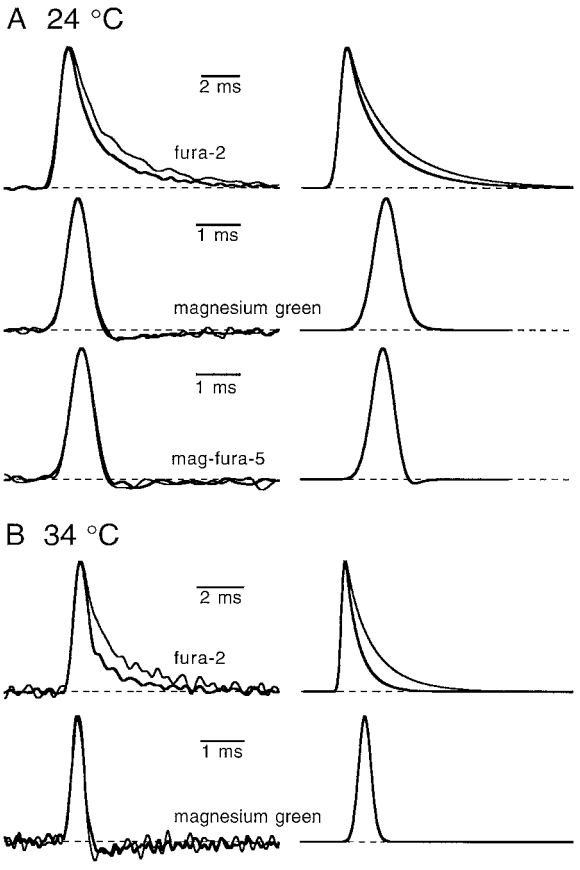

FIGURE 7 Effects of indicator concentration on stimulus-evoked fluorescence transients. (*Left*) Stimulus-evoked fluorescence transients from parallel fibers loaded for 30 min (*thick lines*) or for 5 min (*thin lines*) with the indicated fluorophore at 24°C (*A*) or at 34°C (*B*). (*Right*) Simulation of d[CaF]/d*t* in control conditions (*thin line*) or with the indicator concentration increased (*thick lines*). Concentrations of indicator used in the simulations at 24°C were 18 μM and 30 μM for fura-2, 30 μM and 60 μM for magnesium green and mag-fura-5, and those used in the simulations at 34°C were 20 μM and 40 μM for fura-2, and 30 μM and 60 μM for magnesium green and mag-fura-5.

amount of indicator loaded for fura-2, but not for magnesium green fluorescence transients. Because of the small signal size, it was not possible to measure the derivative of fluorescence transients at 34°C from slices that had been loaded for only 5 min with mag-fura-5. The experimental results of Figs. 6 and 7 were consistent with simulations based on the parameters listed in Table 1.

The time courses of the stimulus-evoked fluorescence transients from magnesium green and mag-fura-5-loaded slices are not limited by the kinetics of the indicator's calcium binding reaction. Therefore the time course of the fluorescence signal from these indicators is determined by the rate of calcium influx. For convenience, in the remainder of the paper we will refer to the derivative of the fluorescence transient of mag-fura-5 or magnesium green as the optically determined calcium current (I_{Ca}^{opt}). In contrast, at both 24°C and 34°C, the time courses of fura-2 fluorescence transients are limited by indicator kinetics and cannot be used to estimate I_{Ca}^{pre}.

Filtering

To maximize the signal-to-noise ratio when recording I_{Ca}^{opt}, we determined the maximum electrical filtering that would not alter its time course. The response of the photodiode used to monitor fluorescence to a 500-μs LED light pulse is shown in Fig. 8 *A*. It shows a slight overshoot (<5%) and has a rising phase limited by a 7–8-kHz corner frequency. We recorded I_{Ca}^{opt} at 24°C and 34°C with magnesium green, without any filtering beyond that imposed by our photodiode, and then digitally filtered off-line. As shown in Fig. 8, at 24°C the shape and amplitude of I_{Ca}^{opt} could be accu-

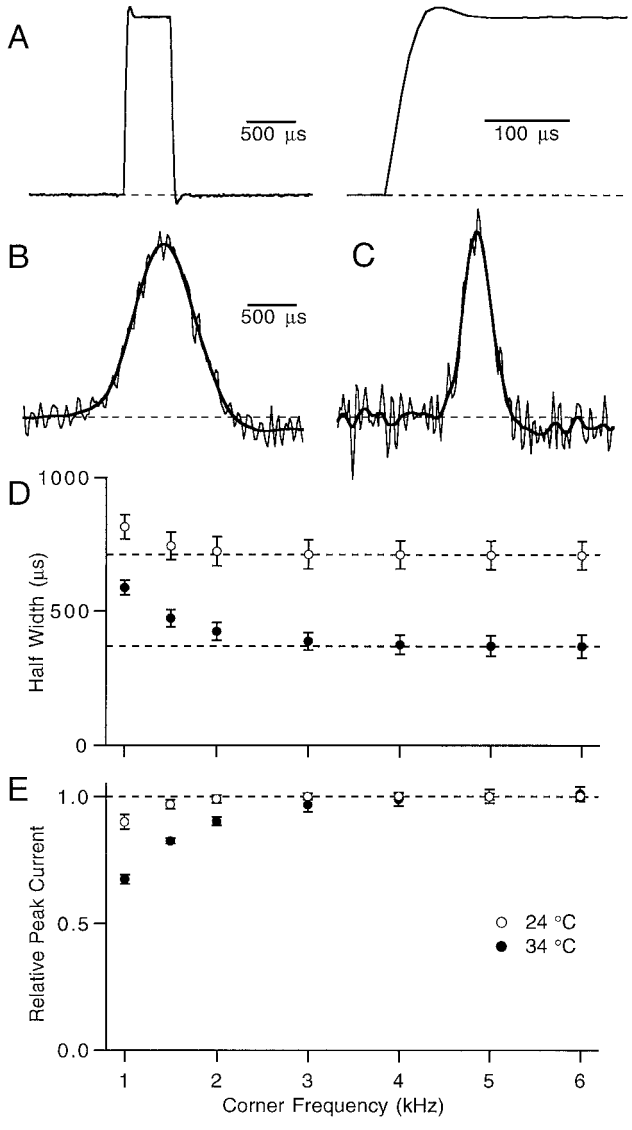

FIGURE 8 The effect of bandwidth on I_{Ca}^{opt}. (*A*) Response of the fluorescence detector to a light pulse from an LED (*left*) and the rising phase of the response on an expanded time scale (*right*). (*B* and *C*) Unfiltered magnesium green I_{Ca}^{opt} (*thin trace*) with a superimposed, digitally filtered version (*thick line*) at 24°C (*B*) or 34°C (*C*). Corner frequencies of 2 kHz and 4 kHz were used at 24°C and 34°C, respectively. (*D* and *E*) The effect of filter corner frequency on I_{Ca}^{opt} half-width (*D*) and peak amplitude (*E*) at 24°C (*open circles*) and 34°C (*filled circles*) (average ± SEM, $n = 5$).

rately recorded with filtering as low as 2 kHz, whereas at 34°C a 3–4-kHz corner frequency was necessary.

Spot size

The fluorescence signal we measured was generated by presynaptic calcium influx triggered by an action potential propagating across the region in the molecular layer, from which we collected light. Therefore, it is important to determine how the time course of I_{Ca}^{opt} is affected by the propagation time of the action potential across the illumination spot. The effect of varying the diameter of the illumination spot on the half-width of I_{Ca}^{opt} is shown in Fig. 9. From the fits to the summary data, we estimate that I_{Ca}^{opt} determined by using a 10-μm spot is ~5% broader than the calcium current at 24°C and 34°C.

Stimulus duration

We record fluorescence changes from a large number of presynaptic terminals located on different axons. To determine if asynchrony in the firing of axons artificially broadens I_{Ca}^{opt}, we examined the effect of varying the stimulus duration (Fig. 10). Remarkably, the firing of the fibers appears to be synchronized to the end of the stimulus pulse.

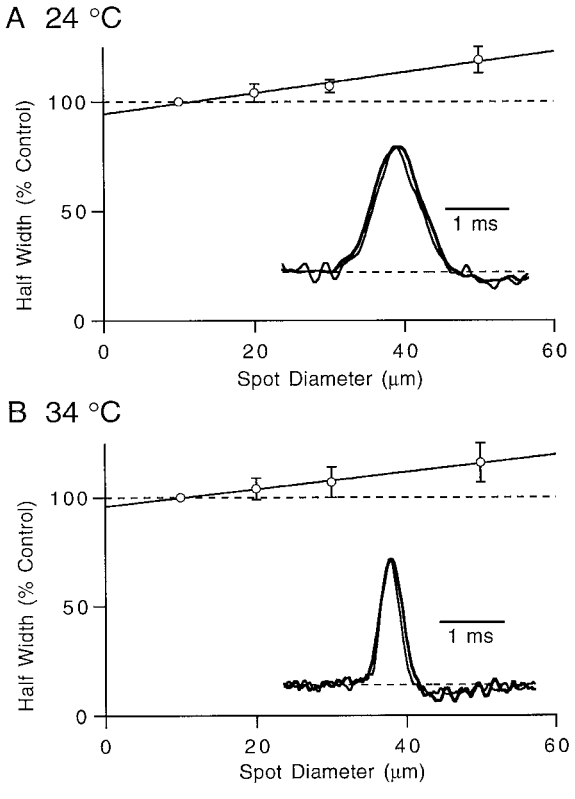

FIGURE 9 The effect of recording spot size on I_{opt}^{Ca}. The width at half maximum of I_{Ca}^{opt} as a function of illumination spot size at 24°C (*A*) or at 34°C (*B*). The half-width for the 10-μm spot was used as control. (*Inset*) Recordings of I_{opt}^{Ca} from a 10-μm (*thin trace*) and a 50-μm (*thick trace*) diameter spot (average ± SEM, $n = 4$).

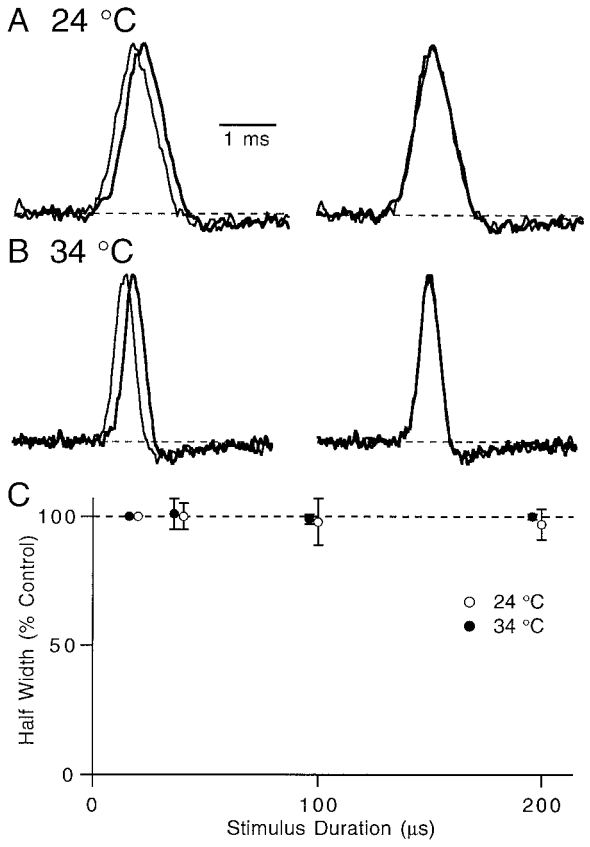

FIGURE 10 The effect of stimulus pulse duration on I_{opt}^{Ca}. (*Left*) I_{opt}^{Ca} recorded after a stimulus pulse of either 20 μs (*thin trace*) or 200 μs (*thick trace*) duration at 24°C (*A*) and 34°C (*B*). (*Right*) The 200-μs trace has been shifted to the left by 180 μs for comparison to the 20-μs trace. (*C*) Summary of the effects of stimulus duration on I_{opt}^{Ca} half-width for recordings at 24°C (*open circles*) and 34°C (*filled circles*). The stimulus durations used were 20, 40, 100, and 200 μs, and I_{opt}^{Ca} after the 20-μs stimulation was used as the control (average ± SEM, $n = 4$).

At both 24°C and 34°C, I_{Ca}^{opt} elicited by stimuli of 20 μs or 200 μs duration had identical time courses, with the exception that the 200 μs current was shifted later by 180 μs. On average, the half-width of I_{Ca}^{opt} was independent of stimulus duration.

Timing of synaptic transmission

To illustrate the utility of the optical detection of the presynaptic calcium current, we simultaneously measured I_{Ca}^{opt}, the presynaptic action potential waveform, and postsynaptic currents at the granule cell to stellate cell synapse at 34°C (Fig. 11). Significant calcium entry occurs during the rising phase of the action potential, and the calcium current reaches ~65% of its maximum amplitude by the peak of the action potential. In addition, because the delay from the start of presynaptic calcium influx to the EPSC is only 180 μs, postsynaptic currents appear before the end of the presynaptic action potential (Sabatini and Regehr, 1996).

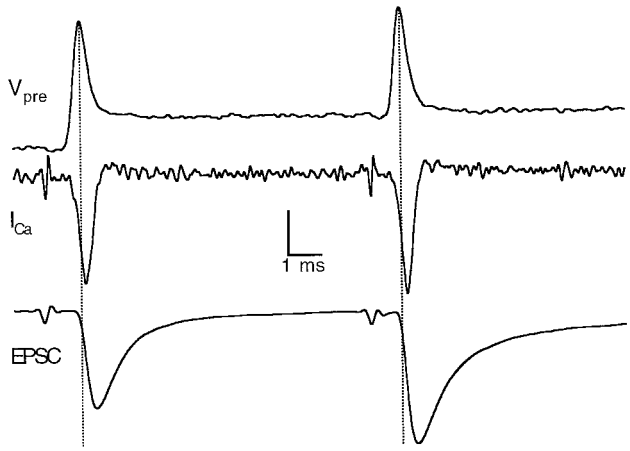

FIGURE 11 Simultaneous recording of presynaptic action potential waveform, presynaptic calcium current, and postsynaptic currents at 34°C in a slice labeled with the voltage-sensitive dye RH482 and the calcium indicator magnesium green. Transmittance transient of RH482 (*top*), magnesium green I_{opt}^{Ca} (*middle*), and voltage-clamped EPSC (*bottom*) from a stellate cell centered in the illumination spot are shown. Two stimuli of 100 μs duration and separated by 10 ms were delivered to the parallel fibers. The vertical scale bar corresponds to 0.1% $\Delta T/T$, 3 (% $\Delta F/F$)/ms, and 100 pA.

DISCUSSION

By theoretically examining a system containing two calcium buffers, we established the conditions required to detect presynaptic calcium currents optically. We found experimentally that low-affinity calcium indicators can provide an accurate measure of the calcium current in presynaptic boutons of cerebellar granule cells. In this discussion we will deal with general issues regarding the optical measurement of presynaptic calcium current and then turn to the application of this approach to granule cell presynaptic boutons.

Theoretical foundation for the optical measurement of presynaptic calcium currents

To evaluate the use of calcium indicators in measuring presynaptic calcium currents, it is crucial to understand the complexities of calcium signaling within a presynaptic terminal. Simulations were invaluable in this regard. We found that spatial gradients of free calcium do not significantly affect the time course of total calcium bound to the indicator within the bouton (Fig. 4). This allowed us to greatly simplify our analysis by treating the presynaptic terminal as a single compartment. We then analyzed the differential equations describing a presynaptic terminal that contained two buffers corresponding to the endogenous buffer and the indicator (see Appendix and Results). Simple analytical approximations were derived that provided insight into the behavior of such a two-buffer system. In response to a step change in calcium concentration, the buffers bind calcium with time courses that are well approximated by the sum of two exponentials with time constants τ_{fast} and τ_{slow}. As shown in the Appendix, τ_{fast} is faster than the equilibration time constant of either buffer alone, and thus the initial response of each buffer is accelerated by the presence of the second buffer. The relative contribution of the fast exponential to the responses of the buffers is determined by $[F]_\infty k_+^F/[B]_\infty k_+^B$ such that, if the ratio is greater than 1, the fast exponential will make a larger contribution to the response of the indicator than to that of the endogenous buffer. When the ratio is less than 1, the converse is true. This component represents the rapid binding of calcium by both buffers until one of them reaches equilibrium with free calcium. Calcium must then transfer from the rapidly equilibrating buffer to the other for the system to reach steady state. The time constant of this process, τ_{slow}, is slower than the time constant of either buffer alone. Because the slow component represents the transfer of calcium from one buffer to the next, its contribution to the response of each buffer is equal and opposite. The slow component becomes more prominent as the difference in the calcium dissociation rates of the buffers increases.

Requirements for accurate optical detection of presynaptic calcium currents

From the general treatment of the two-buffer system, we obtained the conditions necessary for the derivative of the fluorescence change triggered by an action potential to be a good estimate of the time course of the calcium current. The simplest situation is one in which there is very little, if any, endogenous buffer. For this condition, the equilibration rate of the indicator is given by Eq. 8, according to which the calcium-indicator equilibration rate can be made arbitrarily fast by increasing the concentration of the indicator. Even for buffers with slow dissociation rates, like fura-2, only modest concentrations of indicator are required to achieve sufficient speed to follow I_{Ca}^{pre} accurately (Fig. 5 *A*).

More generally, the properties of the endogenous buffer must be taken into account. The presence of an endogenous buffer can profoundly influence the time course of calcium binding to the indicator such that Eq. 8 no longer applies. This is illustrated by Fig. 5 *B*, in which the presence of an endogenous buffer slows the response of fura-2 and makes it virtually impossible to introduce sufficient fura-2 to measure I_{Ca}^{pre} accurately. The presence of the endogenous buffer also influences the interaction of magnesium green and mag-fura-5 with calcium, and it has a beneficial effect by accelerating the calcium binding rate of the indicator (Fig. 5 *B*). However, in other terminals in which the calcium dissociation rate of the endogenous buffer might be different, magnesium green and mag-fura-5 may no longer be suitable for the detection of I_{Ca}^{pre}. This is illustrated by the simulations of Fig. 12. For most of the simulations in the paper, the off rate of the endogenous buffer is 5000 M^{-1} s^{-1}, which is between that of magnesium green ($k_- = 3500$ M^{-1} s^{-1}) and mag-fura-5 ($k_- = 10{,}000$ M^{-1} s^{-1}). Under these conditions, magnesium green and mag-fura-5 both provide a

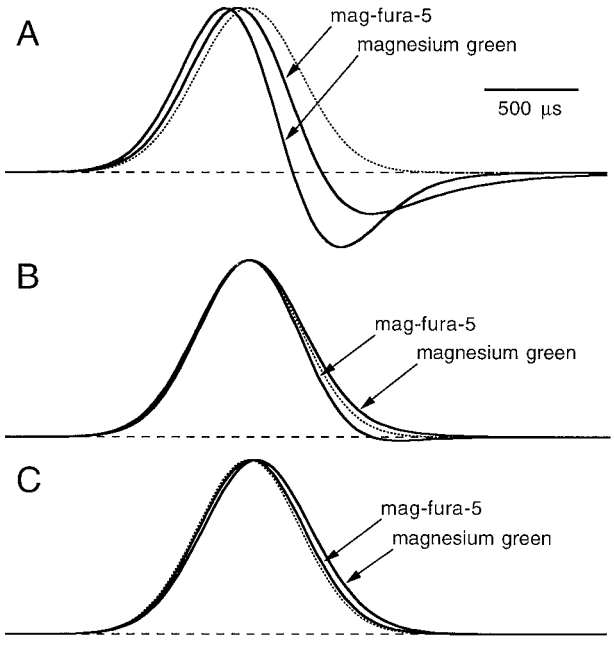

FIGURE 12 Effects of varying the endogenous buffer calcium dissociation rate. Simulations of d[CaF]/dt for mag-fura-5 and magnesium green in the presence of an endogenous buffer with a calcium dissociation rate of 1000 M^{-1} s^{-1} (*A*), 5000 M^{-1} s^{-1} (*B*), or 15,000 M^{-1} s^{-1} (*C*). The dotted line shows the true calcium current. The concentration of indicator used was 100 μM.

good measure of the presynaptic calcium current. When the off rate of the endogenous buffer is decreased to 1000 M^{-1} s^{-1}, there is a large interaction between the indicator and the endogenous buffer, and magnesium green and mag-fura-5 distort the calcium current and report different time courses. With an endogenous buffer with a calcium dissociation rate of 15,000 M^{-1} s^{-1}, magnesium green and mag-fura-5 again provide good measures of the presynaptic calcium current.

Because the kinetic parameters of endogenous calcium buffers are generally not known, it is difficult to match the calcium dissociation rate of the calcium indicator to that of the endogenous buffer. Fortunately, it is possible to test empirically the fidelity with which optical signals report the presynaptic calcium current. As shown in Fig. 12, when the time courses of the endogenous buffer distort the time course of the optical signals, the mag-fura-5 and magnesium green traces are no longer similar in time course. Thus comparing the time course of optical signals from several different indicators with different calcium affinities provides important information on the accuracy of I_{Ca}^{opt}. In addition, if the time course of the fluorescence transient is dependent on the amplitude of calcium influx (Fig. 6 *A*) or the concentration of the indicator (fura-2 traces in Figs. 5 and 7), then the time course of calcium binding to the indicator is limited either by the kinetic parameters of the indicator or by an interaction between the indicator and endogenous buffer, and the indicator will be unsuitable for measuring calcium currents.

Optical detection of presynaptic calcium currents in granule cell presynaptic boutons

We assessed our ability to measure I_{Ca}^{pre} optically in granule cells. Several lines of evidence indicated that fura-2 distorted the calcium current: the time course of the derivative of the stimulus-evoked fluorescence change was much slower than that of low-affinity indicators and was altered by reducing calcium influx or increasing the concentration of fura-2. In contrast, both magnesium green and mag-fura-5 appeared to be well suited to measuring presynaptic calcium currents from granule cells. The derivatives of the stimulus-evoked fluorescence transients of these indicators had the same time course, indicating that interactions with the endogenous buffer did not dominate the kinetics of the response. Furthermore, decreasing calcium entry or increasing the concentrations of these two indicators did not affect the time course of the fluorescence changes, indicating that the rate of rise of fluorescence was not limited by the calcium binding kinetics.

Although the derivatives of the magnesium green and mag-fura-5 fluorescence transients appear to provide good measures of the time course of the presynaptic calcium current, they show small overshoots. It is unlikely that this is a result of interactions between the endogenous buffer and the indicator (as in Fig. 12), for several reasons: 1) the size and time course of the overshoot are the same for the two indicators; 2) the overshoot lasts ~3–4 ms, which is much longer than the duration predicted for interactions between these indicators and the endogenous buffer (see Fig. 14); and 3) the magnitude of the overshoot is unaffected by indicator concentration. A more likely explanation for the overshoot is that it reflects rapid calcium extrusion from the cytoplasm; the time course of fluorescence changes is not only determined by calcium influx through ionic channels, but is sensitive to all changes in calcium levels, including those mediated by the calcium ATPase and Na/Ca exchanger in the plasma membrane and internal stores. As a result of this rapid component of calcium clearance, it will be difficult to optically measure long-lasting components of calcium influx.

Experimental conditions required for optical detection of presynaptic calcium current

In several preparations, including the cerebellar parallel fibers, hippocampal mossy fibers, and hippocampal CA3 to CA1 projections, it is possible to load many presynaptic terminals simultaneously with calcium-sensitive indicators (Feller et al., 1996; Regehr and Atluri, 1995; Regehr and Tank, 1991a,b; Wu and Saggau, 1994). To use the fluorescence changes from such aggregates of en passant synapses to infer the time course of the calcium currents, it is necessary to perform several additional controls. We demonstrate that the propagation time of the action potential across small (<20-μm diameter) spots in the parallel fibers does not broaden the calcium current by more than 10% and that

asynchrony of firing of the axons does not significantly affect the time course of our measurements. In addition, we show that the bandwidth of our fluorescence detector surpasses that necessary to follow calcium currents accurately at both 24°C and 34°C.

Time course and timing of presynaptic calcium entry

The calcium current in granule cell presynaptic boutons was well approximated by a Gaussian with a half-width of 650 μs at 24°C and 340 μs at 34°C. At 24°C the shape of this calcium current is similar to that observed in granule cell bodies and is consistent with simulations of calcium transients using parameters based on calcium channels from granule cells (Sabatini and Regehr, 1997; Wheeler et al., 1996). At 34°C the decrease in calcium current duration is expected as a consequence of faster calcium channel kinetics and the shorter duration of the action potential (McAllister-Williams and Kelly, 1995; Nobile et al., 1990). The shape of the calcium current observed at 34°C is also consistent with simulations based on reported properties of voltage-gated calcium channels (data not shown). An interesting aspect of the observed calcium current at 34°C is that there is significant calcium entry before the peak of the action potential (Fig. 11) (Sabatini and Regehr, 1996). Electrical recordings of calcium currents in Purkinje cells produced by an action potential-like waveform also show that at 35°C calcium currents are extremely rapid and significant calcium influx is observed at the peak of the action potential (McDonough et al., 1997). Synaptic transmission driven by this rapid calcium influx is sufficiently fast to cause a response in the postsynaptic cell, even while the presynaptic bouton is still depolarized (Fig. 11). Based on theoretical considerations, optical measurements of presynaptic calcium entry are expected to report the onset of calcium entry with remarkably high fidelity. Because of the presence of the endogenous buffer, the magnesium green signal should lag the calcium current by less than 10 μs.

APPENDIX: RESPONSE KINETICS OF A TWO-BUFFER SYSTEM TO A STEP CHANGE IN [Ca]

In a system of multiple calcium buffers, the response of an indicator to a change in free calcium concentration is complicated by interactions between the buffers. This is demonstrated in Fig. 13, which shows the concentrations of the calcium-bound form of fura-2 and the endogenous buffer after a step increase in free calcium from 50 nM to 350 nM (see Table 1 for model parameters). The time course of calcium binding for each of the two buffers is different from the exponential increase predicted for the behavior of a single buffer interacting with calcium. The endogenous buffer binds calcium very quickly, but then slowly releases ~30% of it. The fura-2 response, on the other hand, is monotonic, with a small rapid component and a large slow component of calcium binding. To provide a more quantitative description of the dynamics of calcium binding in a system with two buffers and to understand when these interactions will be an important determinant of the time course of calcium binding by an indicator, we develop an analytical approximation to the step response of the two-buffer system.

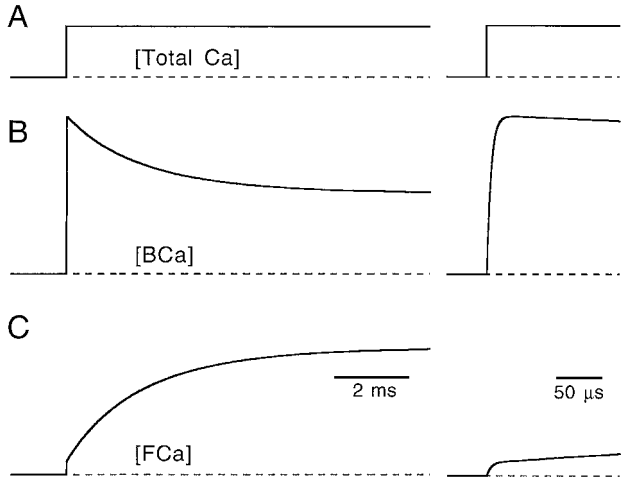

FIGURE 13 Example of calcium binding in a two-buffer system. After a step increase in calcium concentration (*A*), the endogenous buffer quickly binds calcium and then slowly releases ~30% of it (*B*), while fura-2 slowly and monotonically binds calcium (*C*). On the right, the same traces are shown on an expanded scale.

Derivation of analytical approximation

The differential equations that describe calcium binding in a system of two buffers are nonlinear (see Methods, Eqs. 1–3). However, we can derive a linear approximation to the solution to these equations that captures the basic behavior of calcium binding in a system of two buffers and is accurate over a wide range of parameters. Using the definitions

$$u = [\mathrm{BCa}] - [\mathrm{BCa}]_\infty$$

$$v = [\mathrm{FCa}] - [\mathrm{FCa}]_\infty$$

we can rewrite the differential equations governing calcium buffer (Eq. 1) as

$$\frac{1}{k_+^{\mathrm{B}}}\frac{du}{dt} = \frac{1}{k_+^{\mathrm{B}}}\frac{d[\mathrm{BCa}]}{dt}$$

$$= u^2 + uv - u([\mathrm{B}]_\infty + [\mathrm{Ca}]_\infty + K_{\mathrm{d}}^{\mathrm{B}}) - v[\mathrm{B}]_\infty$$

$$\frac{1}{k_+^{\mathrm{F}}}\frac{dv}{dt} = \frac{1}{k_+^{\mathrm{F}}}\frac{d[\mathrm{FCa}]}{dt}$$

$$= v^2 + uv - v([\mathrm{F}]_\infty + [\mathrm{Ca}]_\infty + K_{\mathrm{d}}^{\mathrm{F}}) - u[\mathrm{F}]_\infty$$

We calculate the Jacobian matrix around $u = 0$, $v = 0$ and approximate the full system by the linearized form:

$$\begin{bmatrix} du/dt \\ dv/dt \end{bmatrix} = \mathbf{J}\begin{bmatrix} u \\ v \end{bmatrix} = -\begin{bmatrix} v_{\mathrm{B}} & [\mathrm{B}]_\infty k_+^{\mathrm{B}} \\ [\mathrm{F}]_\infty k_+^{\mathrm{F}} & v_{\mathrm{F}} \end{bmatrix}\begin{bmatrix} u \\ v \end{bmatrix}$$

in which $v_{\mathrm{X}} = k_-^{\mathrm{X}} + k_+^{\mathrm{X}}([\mathrm{X}]_\infty + [\mathrm{Ca}]_\infty)$ and is the equilibration rate of each buffer after a step change in free calcium concentration when the other buffer is not present. The eigenvalues and corresponding eigenvectors of **J** are

$$\lambda_{2,1} = \frac{1}{2}\left[-(v_{\mathrm{B}} + v_{\mathrm{F}}) \pm \sqrt{(v_{\mathrm{B}} + v_{\mathrm{F}})^2 + 4[\mathrm{B}]_\infty[\mathrm{F}]_\infty k_+^{\mathrm{B}} k_+^{\mathrm{F}} - 4v_{\mathrm{B}}v_{\mathrm{F}}}\right] \quad \text{(A1)}$$

$$\mathbf{E}_{1,2} = \begin{bmatrix} E_{1,2x} \\ E_{1,2y} \end{bmatrix} = \begin{bmatrix} 1 \\ -(\nu_B + \lambda_{1,2})([B]_\infty k_+^B)^{-1} \end{bmatrix} \quad \text{(A2)}$$

and can be used to give the solution to the linear approximation

$$\begin{bmatrix} [BCa] \\ [FCa] \end{bmatrix} = C_1 \begin{bmatrix} 1 \\ E_{1y} \end{bmatrix} e^{-t/\tau_{fast}} + C_2 \begin{bmatrix} 1 \\ E_{2y} \end{bmatrix} e^{-t/\tau_{slow}} + \begin{bmatrix} [BCa]_\infty \\ [FCa]_\infty \end{bmatrix} \quad \text{(A3)}$$

where we have used the definitions

$$\tau_{fast} = \frac{1}{\nu_{fast}} = -\frac{1}{\lambda_1} \quad \text{and} \quad \tau_{slow} = \frac{1}{\nu_{slow}} = -\frac{1}{\lambda_2}$$

The coefficients are determined by the initial conditions and are

$$C_1 = \frac{\Delta[FCa] - E_{2y}\Delta[BCa]}{E_{2y} - E_{1y}}$$

and (A4)

$$C_2 = \frac{\Delta[BCa]E_{1y} - \Delta[FCa]}{E_{2y} - E_{1y}}$$

with $\Delta[BCa] = [BCa]_\infty - [BCa]_0$ and $\Delta[FCa]_\infty = [FCa]_\infty - [FCa]_0$.

We see that after a step change in total calcium concentration, the time courses of [BCa] and [FCa] are described by the sum of two exponentials whose magnitudes are determined by C_1, C_2, E_{1y}, and E_{2y}. The two buffers are coupled in such a way that, despite their possibly very different kinetic parameters, they react to a step change in calcium concentration with a time course that is described by a sum of the same two exponentials. However, the magnitude and the sign of the contribution of the two exponentials to the response of each buffer will differ.

The calcium binding displayed in Fig. 13 can now be readily understood. Because the endogenous buffer has a faster calcium dissociation rate than fura-2, it equilibrates with free calcium more rapidly than does fura-2. As fura-2 continues to bind calcium, the endogenous buffer attempts to clamp the free calcium concentration at a level determined by its affinity for calcium. This process results in fura-2 reaching equilibrium in two stages: first, fura-2 binds a small amount of calcium in a competition with the endogenous buffer; and, second, after the endogenous buffer reaches equilibrium with free calcium, calcium is effectively transferred from the endogenous buffer to fura-2 until both buffers reach steady state.

Estimates of the time constants of the exponentials

We can make further approximations and simply the equations above to understand which parameters are important in determining the time constants of the exponentials and their relative magnitudes. From the linear approximation to the square root in the eigenvalues, we can estimate

$$\nu_{slow} \approx \frac{\nu_B\nu_F - [B]_\infty[F]_\infty k_+^B k_+^F}{\nu_B + \nu_F} \quad \text{(A5)}$$

and

$$\nu_{fast} \approx (\nu_B + \nu_F - \nu_{slow}) \approx \nu_B + \nu_F$$

From these equations, we can show that the slow rate of equilibration is slower than the equilibration rate of either buffer alone, but faster than the limits imposed by the equilibration of a vanishingly small amount of either buffer alone. On the other hand, the fast rate constant of equilibration of the two-buffer system is faster than the rate constant of equilibration of either buffer alone.

Estimates of the relative contribution of the fast and slow exponentials

The coefficients C_1, C_2, E_{1y}, and E_{2y} determine the contributions of the fast and slow components of equilibration to the response of each of the two buffers. Under normal steady-state conditions within a cell, [Ca] $\ll$ [F] and [Ca] $\ll$ [B], so that

$$E_{1y} \approx \frac{[F]_\infty k_+^F}{[B]_\infty k_+^B} \quad \text{(A6)}$$

From Eqs. A3 and A6, we see that the ratio of the magnitude of the fast component in the response of the endogenous buffer to its magnitude in the response of the calcium indicator is given by the ratio of the calcium binding rates of the buffers. In the fast equilibration phase, the two buffers compete to bind calcium, and the buffer with the faster calcium binding rate will bind more.

If the concentration of free calcium is small relative to the concentrations of free buffers, we have

$$E_{2y} \approx -\frac{\nu_B\left(1 + \frac{K_d^B}{[B]_\infty}\right) + \nu_F\left(1 + \frac{K_d^F}{[F]_\infty}\right)^{-1}}{\nu_B + \nu_F} \quad \text{(A7)}$$

For the conditions normally present in a calcium indicator-loaded cell, $K_d^X/[X]_\infty \ll 1$, for both the endogenous buffer and the calcium indicator, giving

$$E_{2y} \approx -1 \quad \text{and} \quad \mathbf{E}_2 \approx \begin{bmatrix} 1 \\ -1 \end{bmatrix}$$

Therefore, the magnitude of the slow component of equilibration will be equal and opposite in the two buffers. This represents the slow process of transferring calcium from one buffer to the other until both are in equilibrium with free calcium. It is interesting to note that because $d[CaB]/dt \approx -d[CaF]/dt$ during this period, the free calcium concentration will be nearly constant, even though neither buffer has reached steady state.

From Eqs. A3 and A4, we can derive an approximation for the fractional contribution of the slow component of equilibration to the response of the fluorophore:

$$f_{slow} = \frac{E_{2y}C_2}{E_{1y}C_1 + E_{2y}C_2} \approx \frac{\nu_B + \lambda_2}{\lambda_1 - \lambda_2}\frac{k_-^F - k_-^B}{k_-^B} \quad \text{(A8)}$$

The larger the difference between the off rates of the endogenous buffer and the indicator, the greater the role played by the interaction between the two buffers in determining the time course of the calcium binding to the indicator. On the other hand, for two buffers with the same off rate, regardless of their concentrations and on rates, no interaction terms will be present. For this reason, the best indicators for optically measuring calcium currents will be those with calcium dissociation rates similar to that of the dominant endogenous calcium buffer.

We can use the approximations above to explain the results of the simulations of the effect of the presence of the endogenous buffer on the fluorescence transients (Fig. 5). The parameters used in our model (see Table 1) reproduce our experimental data (Fig. 2) and are similar to those of the dominant buffer in chromaffin cells (Xu et al., 1997). Because the dissociation rate of fura-2 is more than an order of magnitude smaller than that of the endogenous buffer, the fura-2 fluorescence transient is dominated by the slow component of equilibration. Fig. 14 summarizes the effect of indicator concentration on the kinetics of calcium binding in the presence of the endogenous buffer. Increasing the concentration of fura-2 accelerates the fast and slow time components of equilibration and augments the relative contribution of the fast component to the response of the indicator, $f_{fast} = 1 - f_{slow}$. However, because the fura-2 response is dominated by the slow component, increasing the fura-2 concentration does not accelerate the calcium binding kinetics as much as Eq. 8 predicts.

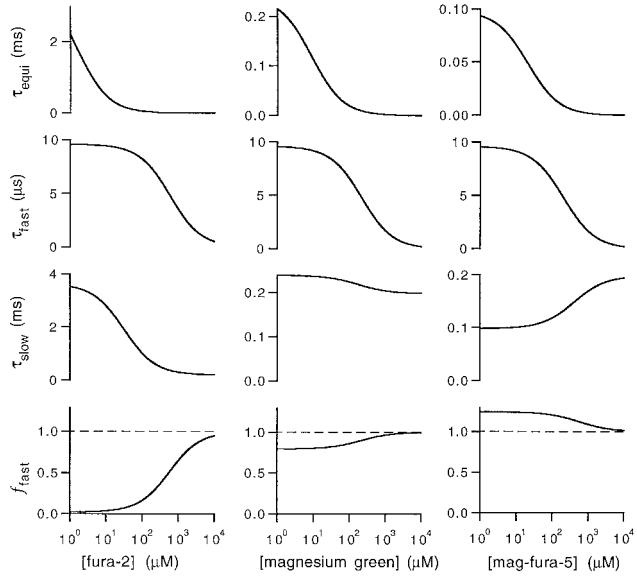

FIGURE 14 Effects of indicator concentration on the time course of calcium binding in the presence of an endogenous buffer. For fura-2, magnesium green, and mag-fura-5, the time constant of equilibration of the indicator when no endogenous buffer is present, the fast and slow time constants of equilibration in the presence of endogenous buffer, and the relative magnitude of the fast component of equilibration in the presence of endogenous buffer are plotted as a function of indicator concentration.

Magnesium green has a dissociation rate slightly less than that of the endogenous buffer, and therefore the slow component of equilibration makes a small contribution and slightly elongates the derivative of magnesium green fluorescence transients compared to the calcium current. Mag-fura-5 has a dissociation constant faster than that of the endogenous buffer and equilibrates more rapidly with calcium. Mag-fura-5 binds calcium past its steady-state concentration and then releases calcium to the endogenous buffer as the system equilibrates. This appears as the overshoot in d[CaF]/d*t* (Fig. 5 *B*) and results in the fast component of equilibration, making a fractional contribution greater than 1 to the response of mag-fura-5.

We thank Pradeep Atluri, Chinfei Chen, Jeremy Dittman, Matthew Friedman, and Bruce Peters for comments on the manuscript.

This work was supported by the National Institutes of Health (R01-NS32405-01), a McKnight Scholars Award, and a Klingenstein Fellowship Award in the Neurosciences to WGR, and by a NEI training grant T32EY07110-06 and a Quan Fellowship to BLS.

REFERENCES

Atluri, P. P., and W. G. Regehr. 1996. Determinants of the time course of facilitation at the granule cell to Purkinje cell synapse. *J. Neurosci.* 16:5661–5671.

Augustine, G. J., and R. Eckert. 1984. Divalent cations differentially support transmitter release at the squid giant synapse. *J. Physiol. (Lond.).* 346:257–271.

Blumenfeld, H., L. Zablow, and B. Sabatini. 1992. Evaluation of cellular mechanisms for modulation of calcium transients using a mathematical model of fura-2 Ca^{2+} imaging in *Aplysia* sensory neurons. *Biophys. J.* 63:1146–1164.

Borst, J. G. G., and B. Sakmann. 1996. Calcium influx and transmitter release in a fast CNS synapse. *Nature.* 383:431–434.

Connor, J. A., and G. Nikolakopoulou. 1982. Calcium diffusion and buffering in nerve cytoplasm. *Lect. Math. Life Sci.* 15:79–101.

Crank, J. 1975. The Mathematics of Diffusion, 2nd Ed. Clarendon Press, Oxford.

Delbono, O., and E. Stefani. 1993. Calcium transients in single mammalian skeletal muscle fibers. *J. Physiol. (Lond.).* 463:689–707.

Dodge, F. A., and R. Rahamimoff. 1967. Co-operative action of calcium ions in transmitter release at the neuromuscular junction. *J. Physiol. (Lond.).* 193:419–432.

Feller, M. B., K. R. Delaney, and D. W. Tank. 1996. Presynaptic calcium dynamics at the frog retinotectal synapse. *J. Neurophysiol.* 76:381–400.

Fogelson, A. L., and R. S. Zucker. 1985. Presynaptic calcium diffusion from various arrays of single channels. Implications for transmitter release and synaptic facilitation. *Biophys. J.* 48:1003–1017.

Grisell, R. D., and M. C. Andresen. 1979. Multicompartment diffusion and reaction modeling system applied to transmitter-mediated photoreception. *Computers Biol. Med.* 9:107–129.

Grynkiewicz, G., M. Poenie, and R. Y. Tsien. 1985. A new generation of Ca^{2+} indicators with greatly improved fluorescence properties. *J. Biol. Chem.* 260:3440–3450.

Haugland, R. P. 1996. Handbook of Fluorescent Probes and Research Chemicals, 6th Ed. Molecular Probes, Eugene, OR.

Helmchen, F., J. G. G. Borst, and B. Sakmann. 1997. Calcium dynamics associated with a single action potential in a CNS presynaptic terminal. *Biophys. J.* 72:1458–1471.

Herrington, J., and R. J. Bookman. 1995. Pulse Control V4.5: IGOR XOPs for Patch Clamp Data Acquisition. University of Miami, Miami, FL.

Jenkinson, D. H. 1957. The nature of the antagonism between calcium and magnesium ions at the neuromuscular junction. *J. Physiol. (Lond.).* 138:434–444.

Kao, J. P. Y., and R. Y. Tsien. 1988. Ca^{2+} binding kinetics of fura-2 and azo-1 from temperature-jump relaxation measurements. *Biophys. J.* 53: 635–639.

Katz, B., and R. Miledi. 1967. The timing of calcium action during neuromuscular transmission. *J. Physiol. (Lond.).* 189:535–544.

Kocsis, J. D., R. C. Malenka, and S. G. Waxman. 1983. Effects of extracellular potassium concentration on the excitability of the parallel fibres of the rat cerebellum. *J. Physiol. (Lond.).* 334:225–244.

Konnerth, A., A. L. Obaid, and B. M. Salzberg. 1987. Optical recording of electrical activity from parallel fibres and other cell types in skate cerebellar slices in vitro. *J. Physiol. (Lond.).* 393:681–702.

Lagnado, L., L. Cervetto, and P. A. McNaughton. 1992. Calcium homeostasis in the outer segments of retinal rods from the tiger salamander. *J. Physiol. (Lond.).* 455:111–142.

Llinas, R., Z. Steinberg, and K. Walton. 1981. Presynaptic calcium currents in squid giant synapse. *Biophys. J.* 33:289–322.

Martin, A. R., V. Patel, L. Faille, and A. Mallart. 1989. Presynaptic calcium currents recorded from calyciform nerve terminals in the lizard ciliary ganglion. *Neurosci. Lett.* 105:14–18.

McAllister-Williams, R. H., and J. S. Kelly. 1995. The temperature dependence of high-threshold calcium channel currents recorded from adult rat dorsal raphe neurones. *Neuropharmacology.* 34:1479–1490.

McDonough, S. I., I. M. Mintz, and B. P. Bean. 1997. Alteration of P-type calcium channel gating by the spided toxin omega-Aga-IVA. *Biophys. J.* 72:2117–2128.

Mintz, I. M., B. L. Sabatini, and W. G. Regehr. 1995. Calcium control of transmitter release at a cerebellar synapse. *Neuron.* 15:675–688.

Neher, E. 1995. The use of fura-2 for estimating Ca buffers and Ca fluxes. *Neuropharmacology.* 34:1423–1442.

Neher, E., and G. J. Augustine. 1992. Calcium gradients and buffers in bovine chromaffin cells. *J. Physiol. (Lond.).* 450:273–301.

Nobile, M., E. Carbone, H. D. Lux, and H. Zucker. 1990. Temperature sensitivity of Ca currents in chick sensory neurones. *Pflugers Arch.* 415:658–663.

Nowycky, M. C., and M. J. Pinter. 1993. Time courses of calcium and calcium-bound buffers following calcium influx in a model cell. *Biophys. J.* 64:77–91.

Palay, S. L., and V. Chan-Palay. 1974. Cerebellar Cortex. Springer Verlag, New York.

Press, W. H., S. A. Teukolsky, W. T. Vetterling, and B. P. Flannery. 1992. Numerical Recipes in C: The Art of Scientific Computation, 2nd Ed. Cambridge University Press, Cambridge.

Regehr, W. G., and P. P. Atluri. 1995. Calcium transients in cerebellar granule cell presynaptic terminals. *Biophys. J.* 68:2156–2170.

Regehr, W. G., and I. M. Mintz. 1994. Participation of multiple calcium channel types in transmission at single climbing fiber to Purkinje cell synapses. *Neuron.* 12:605–613.

Regehr, W. G., and D. W. Tank. 1991a. The maintenance of LTP at hippocampal mossy fiber synapses is independent of sustained presynaptic calcium. *Neuron.* 7:451–459.

Regehr, W. G., and D. W. Tank. 1991b. Selective fura-2 loading of presynaptic terminals and nerve cell processes by local perfusion in mammalian brain slice. *J. Neurosci. Methods.* 37:111–119.

Roberts, W. M. 1993. Spatial calcium buffering in saccular hair cells. *Nature.* 363:74–76.

Roberts, W. M. 1994. Localization of calcium signals by a mobile calcium buffer in frog saccular hair cells. *J. Neurosci.* 14:3246–3262.

Roberts, W. M., R. A. Jacobs, and A. J. Hudspeth. 1990. Colocalization of ion channels involved in frequency selectivity and synaptic transmission at presynaptic active zones of hair cells. *J. Neurosci.* 10:3664–3684.

Sabatini, B. L., and W. G. Regehr. 1995. Detecting changes in calcium influx which contribute to synaptic modulation in mammalian brain slice. *Neuropharmacology.* 34:1453–1467.

Sabatini, B. L., and W. G. Regehr. 1996. Timing of neurotransmission at fast synapses in the mammalian brain. *Nature.* 384:170–172.

Sabatini, B. L., and W. G. Regehr. 1997. Control of neurotransmitter release by presynaptic waveform at the granule cell to Purkinje cell synapse. *J. Neurosci.* 17:3425–3435.

Sala, F., and A. Hernandez-Cruz. 1990. Calcium diffusion modeling in a spherical neuron. *Biophys. J.* 57:313–324.

Schweizer, F. E., H. Betz, and G. J. Augustine. 1995. From vesicle docking to endocytosis: intermediate reactions of exocytosis. *Neuron.* 14: 689–696.

Simon, S. M., and R. R. Llinas. 1985. Compartmentalization of the submembrane calcium activity during calcium influx and its significance in transmitter release. *Biophys. J.* 48:485–498.

Sinha, S. R., L. G. Wu, and P. Saggau. 1997. Presynaptic calcium dynamics and transmitter release evoked by single action potentials at mammalian central synapses. *Biophys. J.* 72:637–651.

Sivaramakrishnan, S., and G. Laurent. 1995. Pharmacological characterization of presynaptic calcium currents underlying glutamatergic transmission in the avian auditory brainstem. *J. Neurosci.* 15:6576–6585.

Smith, S. J., and R. S. Zucker. 1980. Aequorin response facilitation and intracellular calcium accumulation in molluscan neurones. *J. Physiol. (Lond.).* 300:167–196.

Stanley, E. F. 1989. Calcium currents in a vertebrate presynaptic nerve terminal: the chick ciliary ganglion calyx. *Brain Res.* 505:341–345.

Tank, D. W., W. G. Regehr, and K. R. Delaney. 1995. A quantitative analysis of presynaptic calcium dynamics that contribute to short-term enhancement. *J. Neurosci.* 15:7940–7952.

Wheeler, D. B., A. Randall, and R. W. Tsien. 1996. Changes in action potential duration alter reliance of excitatory synaptic transmission on multiple types of Ca^{2+} channels in rat hippocampus. *J. Neurosci.* 16: 2226–2237.

Wu, L.-G., and P. Saggau. 1994. Pharmacological identification of two types of presynaptic voltage-dependent calcium channels at CA3-CA1 synapses of the hippocampus. *J. Neurosci.* 14:5613–5622.

Xu, T., M. Naraghi, H. G. Kang, and E. Neher. 1997. Kinetic studies of Ca^{2+} binding and Ca^{2+} clearance in the cytosol of adrenal chromaffin cells. *Biophys. J.* 73:532–545.

Yawo, H. 1990. Voltage-activated calcium currents in presynaptic terminals of chicken ciliary ganglion. *J. Physiol. (Lond.).* 428:199–213.

Zhao, M., S. Hollingworth, and S. M. Baylor. 1996. Properties of tri- and tetracarboxylate Ca^{2+} indicators in frog skeletal muscle fibers. *Biophys. J.* 70:896–916.

Zhou, Z., and E. Neher. 1993. Mobile and immobile calcium buffers in bovine adrenal chromaffin cells. *J. Physiol. (Lond.).* 469:245–273.